Beam Halo Management

Christopher Mayes – October 20, 2011

Lab FEL viewscreens

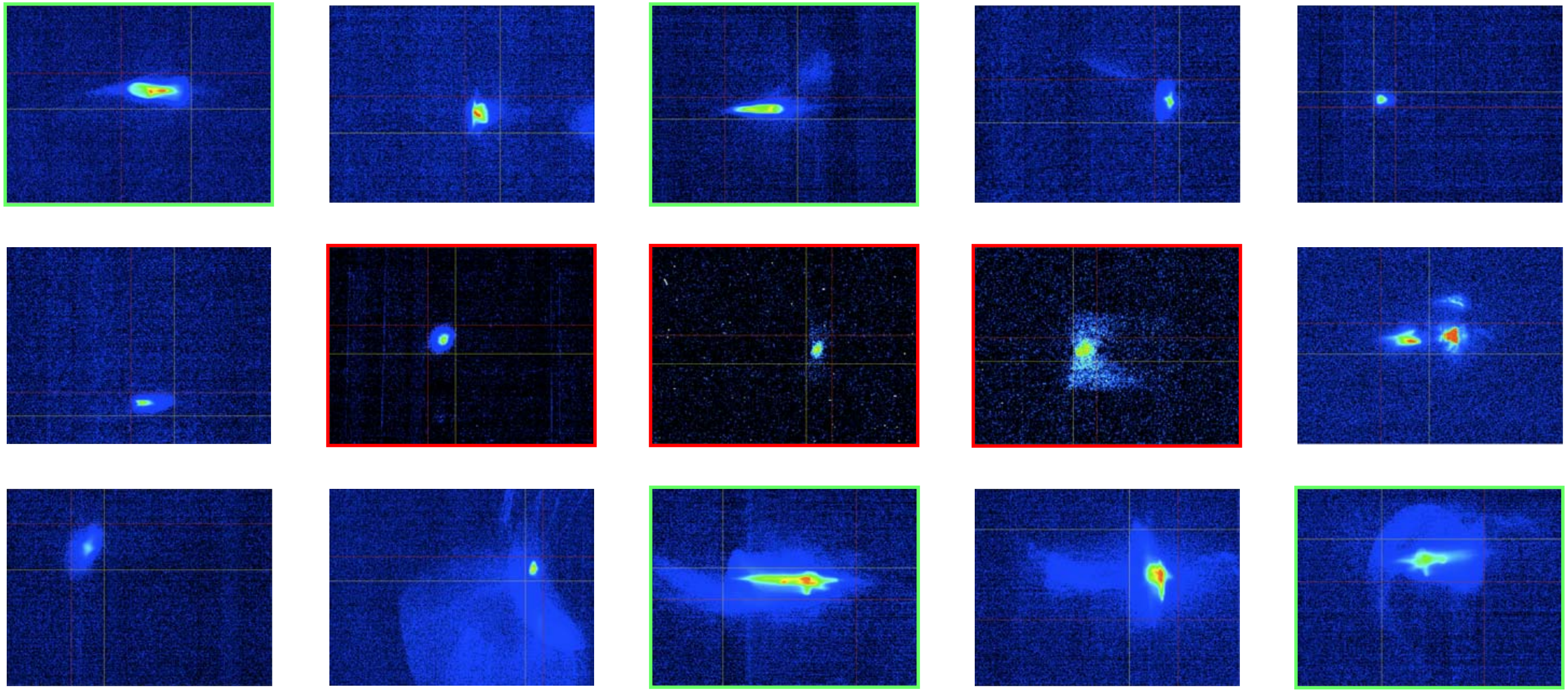

[Courtesy of S. Benson]

BERLinPro simulations (Astra)

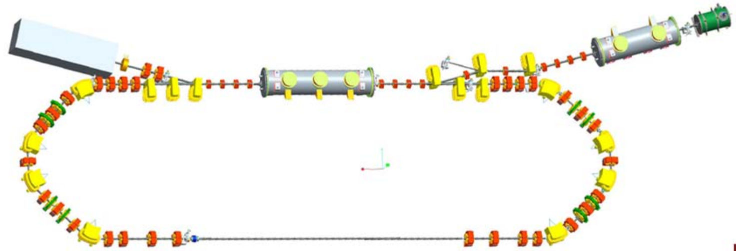

x,y projection

Long. phase space

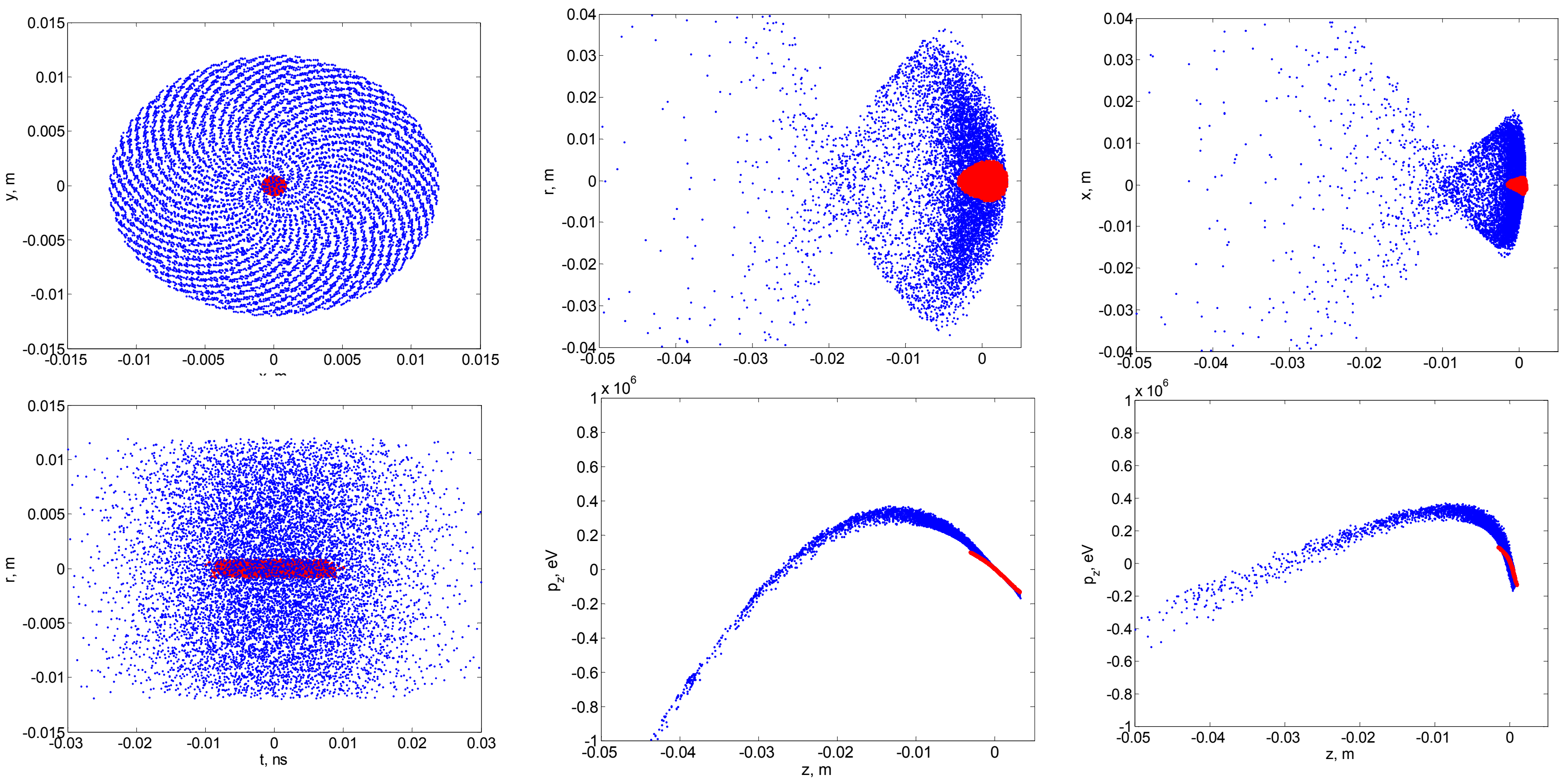

at cathode **after booster** **after dogleg**

[Courtesy of A. Matveenko]

BERLinPro simulations (Astra)

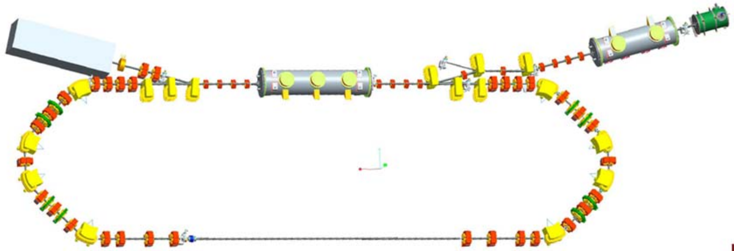

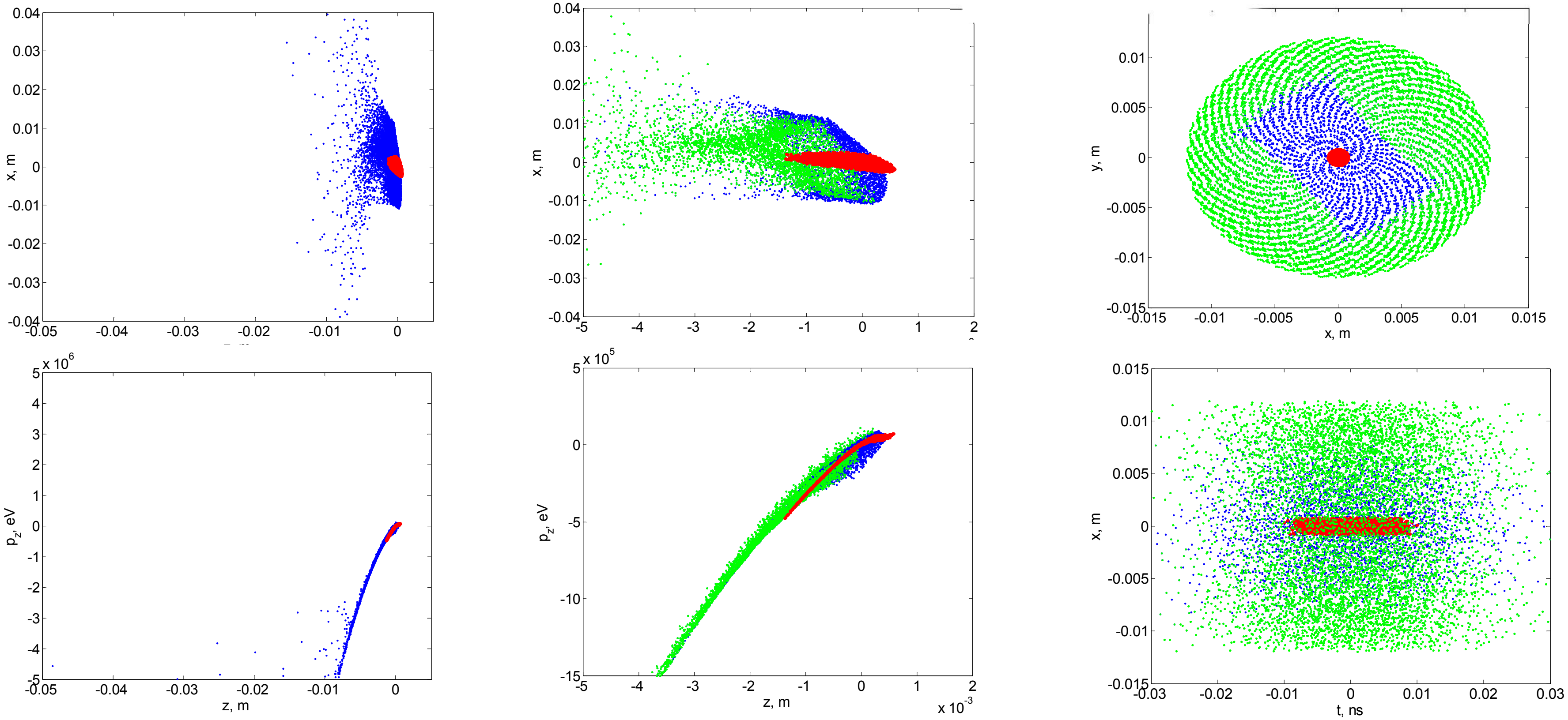

After linac

Particles lost at multiple apertures (0.02 m)

Starting positions at cathode

[Courtesy of A. Matveenko]

Cornell Prototype ERL injector

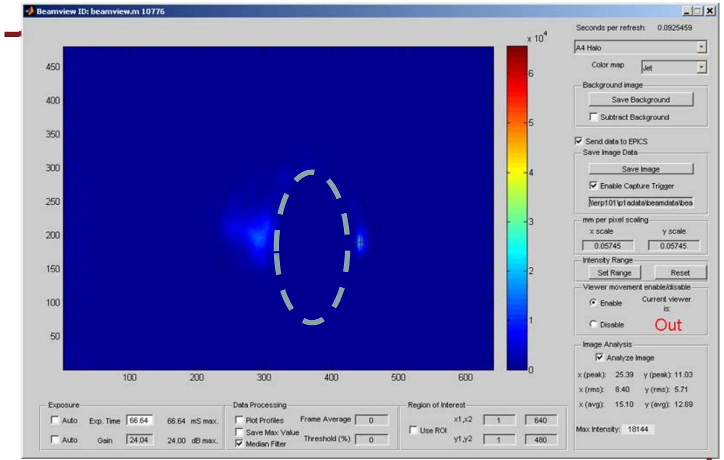

- field emission from the cathode
- field emission from the gun electrodes
- discharges from the gun insulator
- stray light reaching the cathode (big problem for high QE cathodes)
    - sources: room lights, scattered laser light, x-rays/UV light from SRF cavities, x-rays/UV from gun electrode discharges
- field emission from SRF cavities, that gets accelerated and exits the cavity
- space charge?
- non-uniform laser which makes long tails in time or space
- ghost pulses from the laser,
- cathode response time too long which produces tails in time (tails get defocused and become lost or turn into halo)
- ions/ion scattering?

We have seen most of these in our injector and are working to reduce or get rid of them. We now think we have identified the main cause of our halo – poor laser mirrors before the cathode.

[Courtesy of B. Dunham]

However. . .

Even with a perfect beam:

Gas scattering

Intra-beam scattering

Touschek scattering

Dark current from cavity field emission

Touschek Scattering (A. Piwinski 1998)

Scattering probability distribution

$$\begin{aligned}\frac{1}{\sigma_h^2} &= \frac{1}{\sigma_p^2} + \frac{D_x^2 + \tilde{D}_x^2}{\sigma_{x\beta}^2} + \frac{D_z^2 + \tilde{D}_z^2}{\sigma_{z\beta}^2} \\ &= \frac{1}{\sigma_p^2 \sigma_{x\beta}^2 \sigma_{z\beta}^2}\left(\tilde{\sigma}_x^2 \sigma_{z\beta}^2 + \tilde{\sigma}_z^2 \sigma_{x\beta}^2 - \sigma_{x\beta}^2 \sigma_{z\beta}^2\right)\end{aligned} \tag{32}$$

$$B_1 = \frac{\beta_x^2}{2\beta^2\gamma^2\sigma_{x\beta}^2}\left(1 - \frac{\sigma_h^2 \tilde{D}_x^2}{\sigma_{x\beta}^2}\right) + \frac{\beta_z^2}{2\beta^2\gamma^2\sigma_{z\beta}^2}\left(1 - \frac{\sigma_h^2 \tilde{D}_z^2}{\sigma_{z\beta}^2}\right) \tag{33}$$

$$\begin{aligned}B_2^2 &= \frac{1}{4\beta^4\gamma^4}\left(\frac{\beta_x^2}{\sigma_{x\beta}^2}\left(1 - \frac{\sigma_h^2 \tilde{D}_x^2}{\sigma_{x\beta}^2}\right) - \frac{\beta_z^2}{\sigma_{z\beta}^2}\left(1 - \frac{\sigma_h^2 \tilde{D}_z^2}{\sigma_{z\beta}^2}\right)\right)^2 + \frac{\sigma_h^4 \beta_x^2 \beta_z^2 \tilde{D}_x^2 \tilde{D}_z^2}{\beta^4\gamma^4\sigma_{x\beta}^4\sigma_{z\beta}^4} \\ &= B_1^2 - \frac{\beta_x^2\beta_z^2\sigma_h^2}{\beta^4\gamma^4\sigma_{x\beta}^4\sigma_{z\beta}^4\sigma_p^2}\left(\sigma_x^2\sigma_z^2 - \sigma_p^4 D_x^2 D_z^2\right)\end{aligned} \tag{34}$$

$$\tau_m = \beta^2 \delta_m^2 \tag{35}$$

In order to simplify the representation we have introduced

$$\tilde{D}_{x,z} = \alpha_{x,z} D_{x,z} + \beta_{x,z} D'_{x,z} \tag{36}$$

and

$$\tilde{\sigma}_{x,z}^2 = \sigma_{x,z}^2 + \sigma_p^2 \tilde{D}_{x,z}^2 = \sigma_{x\beta,z\beta}^2 + \sigma_p^2 (D_{x,z}^2 + \tilde{D}_{x,z}^2) \tag{37}$$

$$\begin{aligned}R &= \frac{r_p^2 c \beta_x \beta_z \sigma_h N_p^2}{8\sqrt{\pi}\beta^2\gamma^4\sigma_{x\beta}^2\sigma_{z\beta}^2\sigma_s\sigma_p}\int_{\tau_m}^{\infty}\left(\left(2 + \frac{1}{\tau}\right)^2\left(\frac{\tau/\tau_m}{1+\tau} - 1\right) + 1 - \frac{\sqrt{1+\tau}}{\sqrt{\tau/\tau_m}}\right. \\ &\left. - \frac{1}{2\tau}\left(4 + \frac{1}{\tau}\right)\ln\frac{\tau/\tau_m}{1+\tau}\right)e^{-B_1\tau} I_o(B_2\tau)\frac{\sqrt{\tau}\,d\tau}{\sqrt{1+\tau}}\end{aligned} \tag{31}$$

Cornell ERL Layout

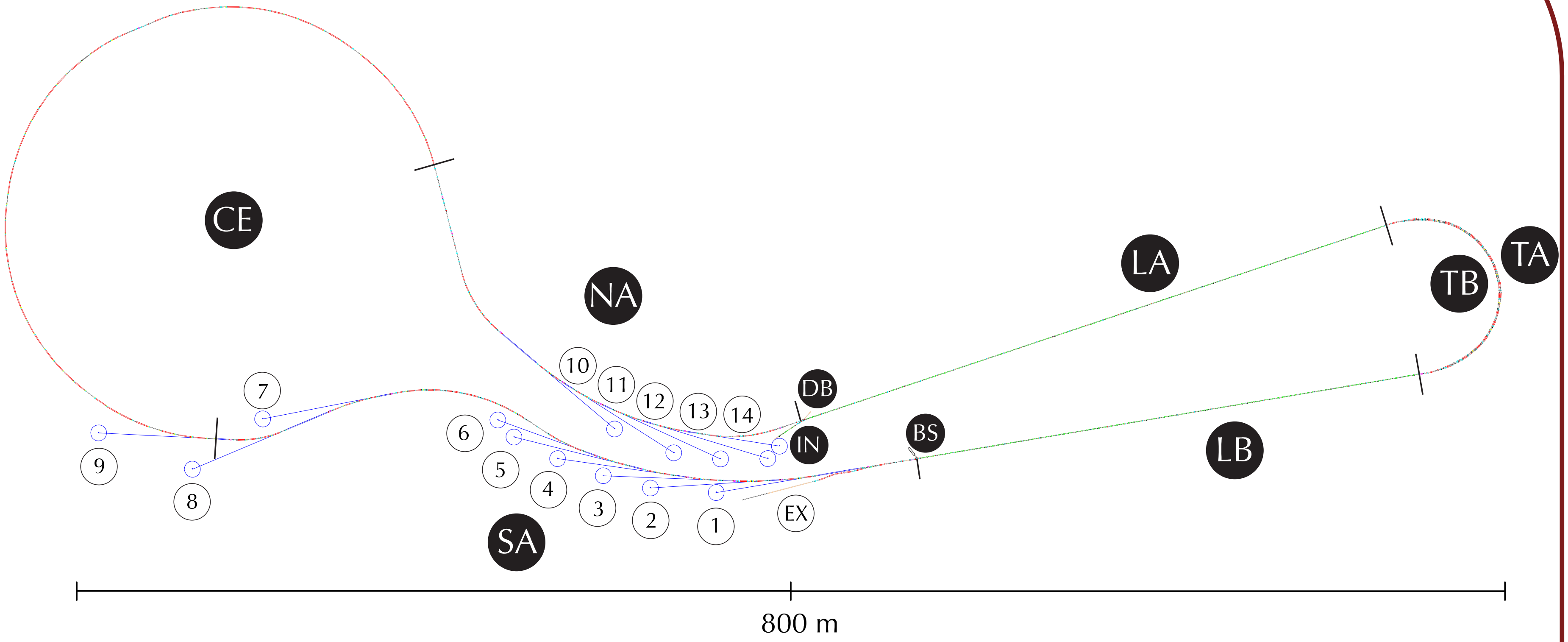

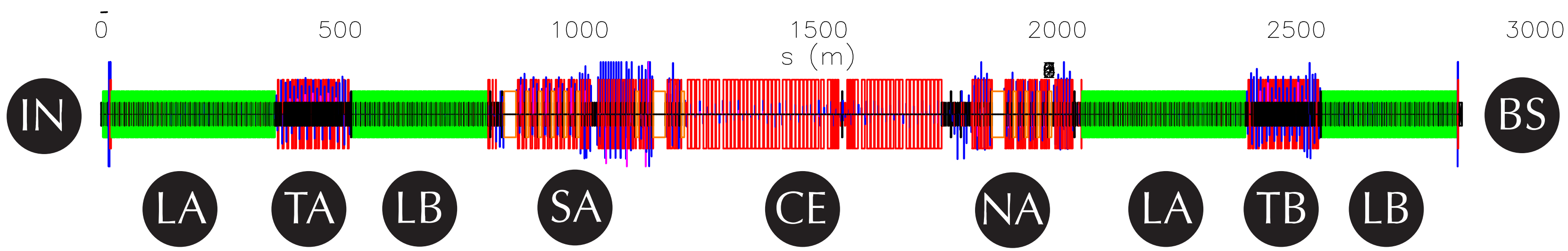

Christopher Mayes – October 20, 2011

Touschek particle

[Code developed by M. Ehrlichman using Bmad (D. Sagan)]

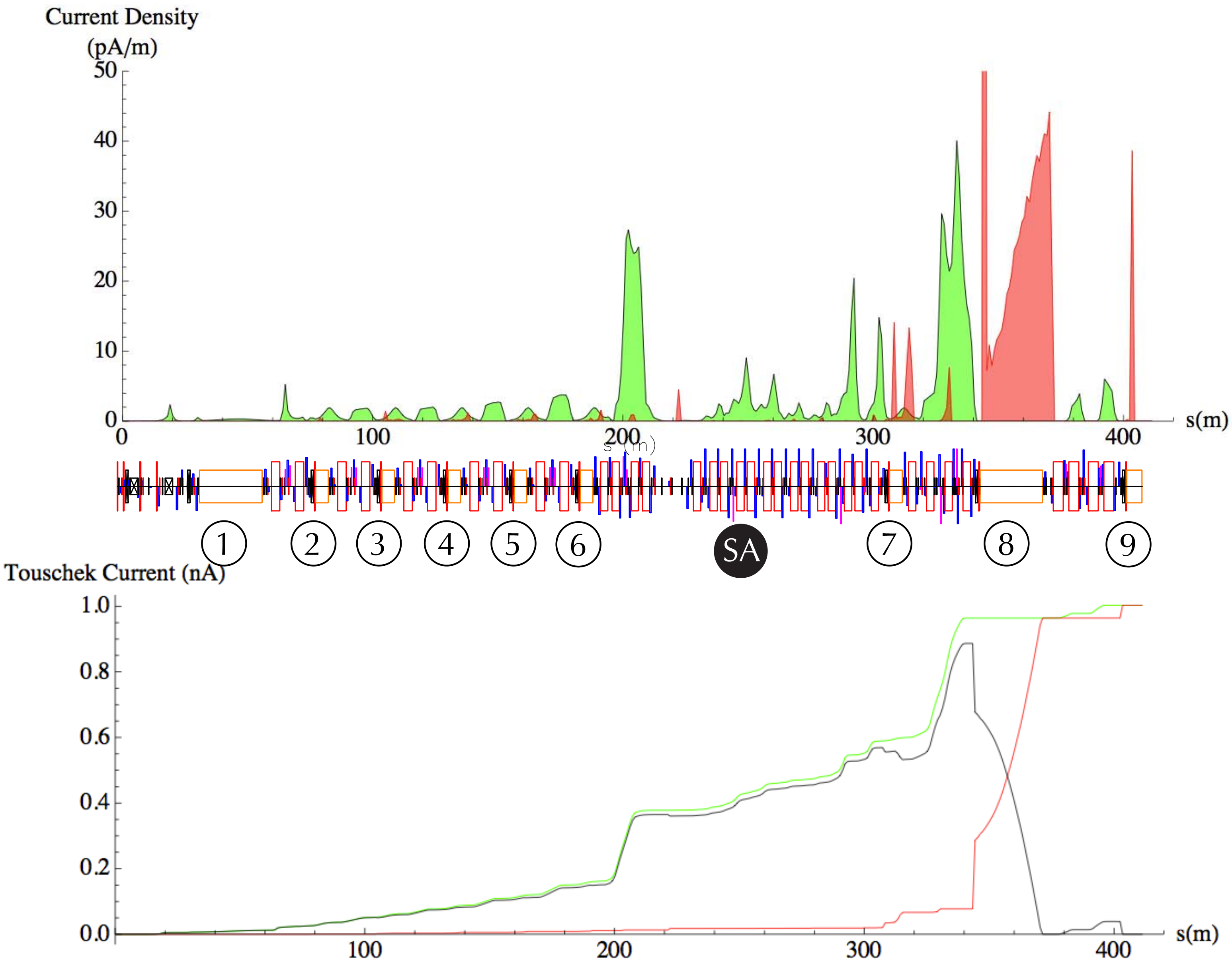

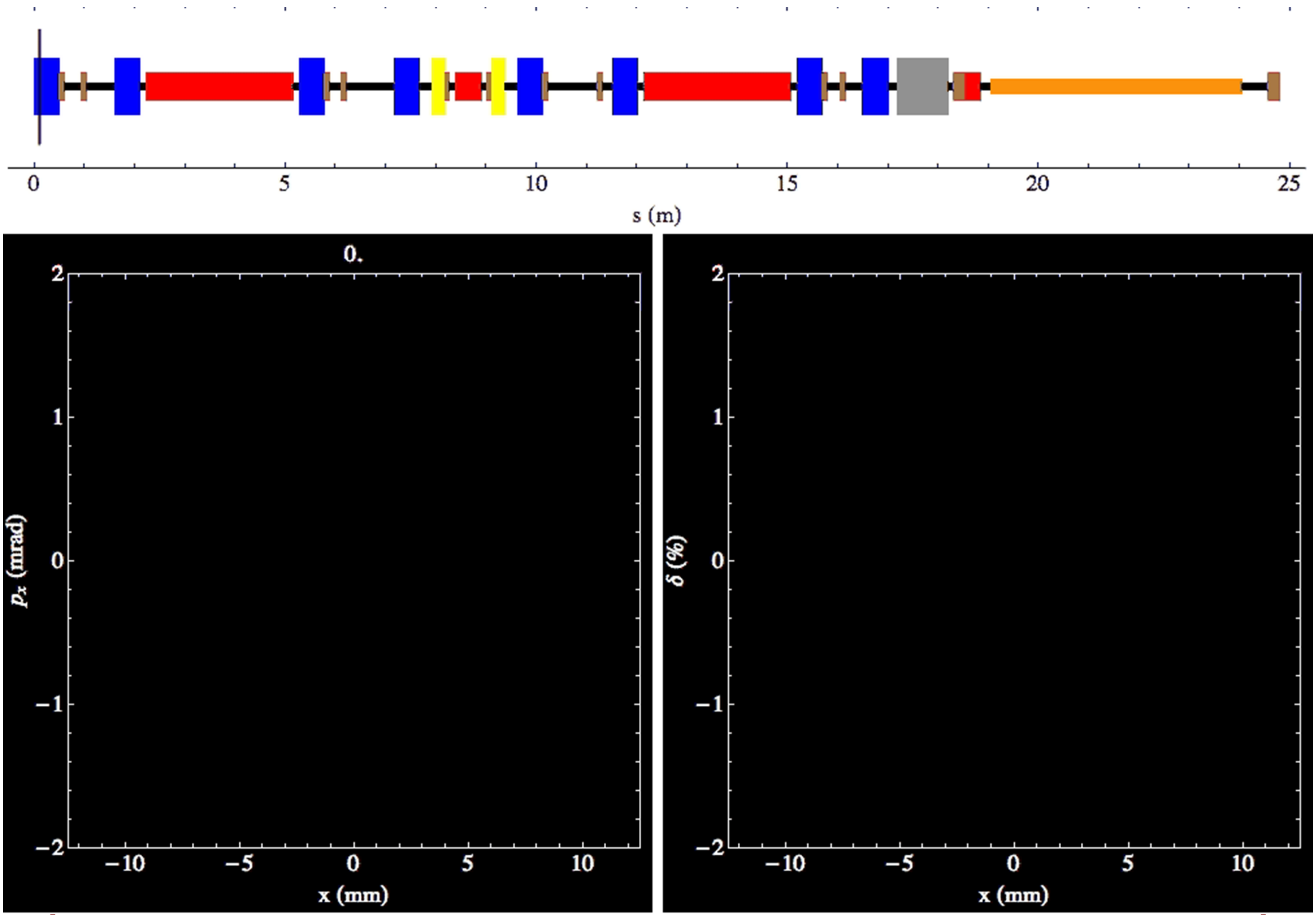
0
5
10
15
20
25
s (m)
0.
2
1
0
−1
−2
p_x (mrad)
−10
−5
0
5
10
x (mm)
δ (%)

Touschek optimization 0

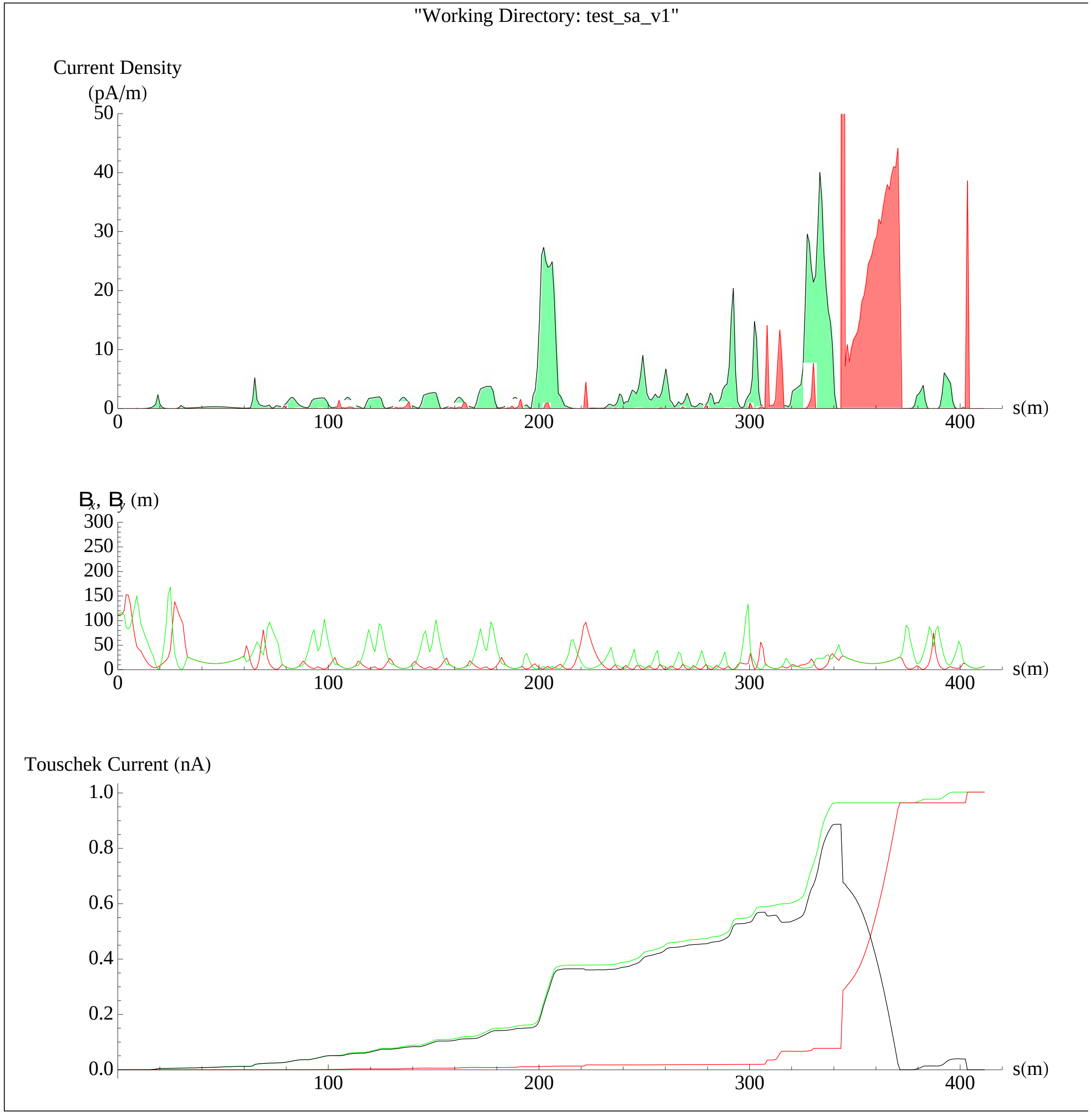

Touschek optimization 1

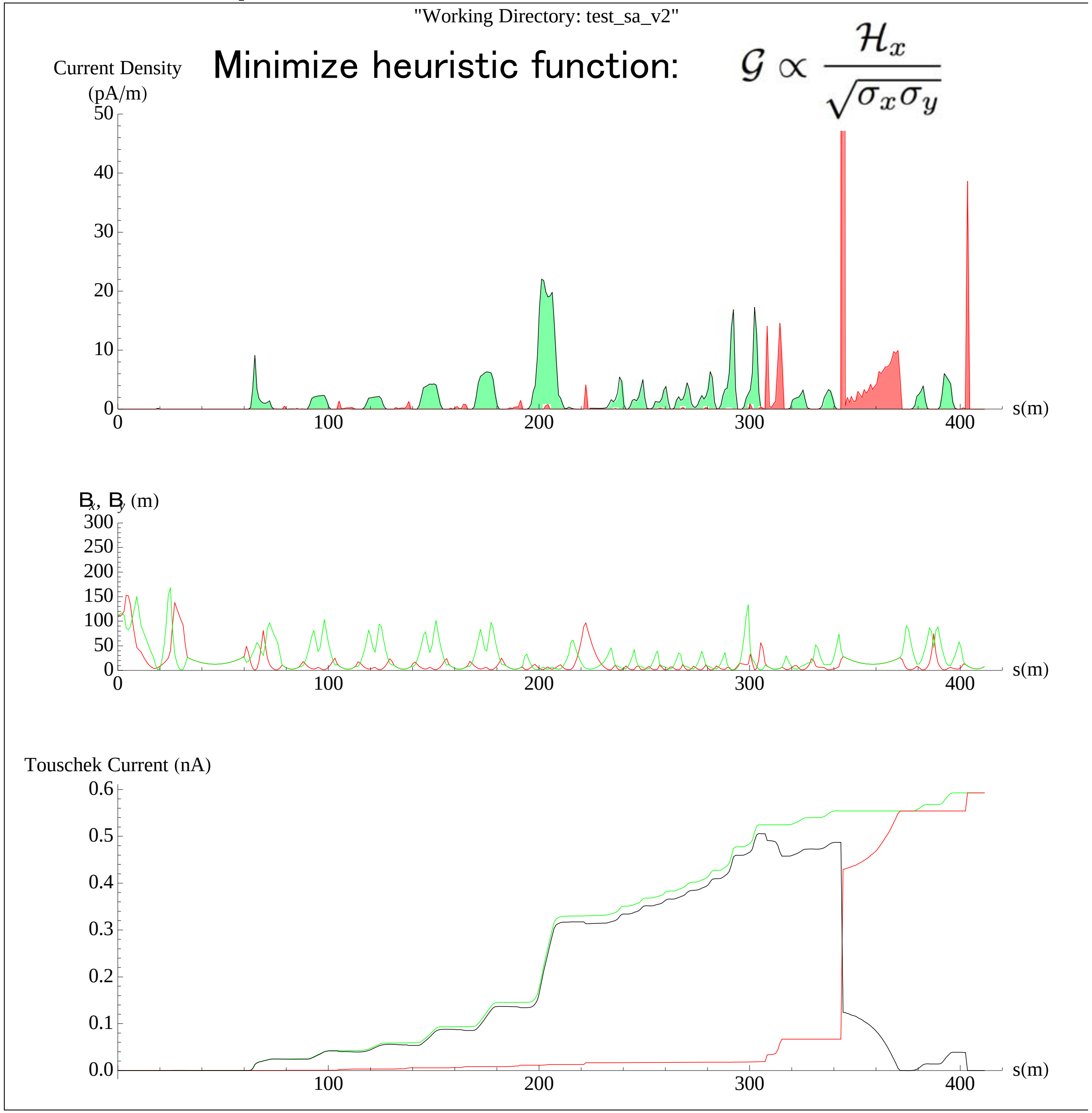

Touschek optimization 2

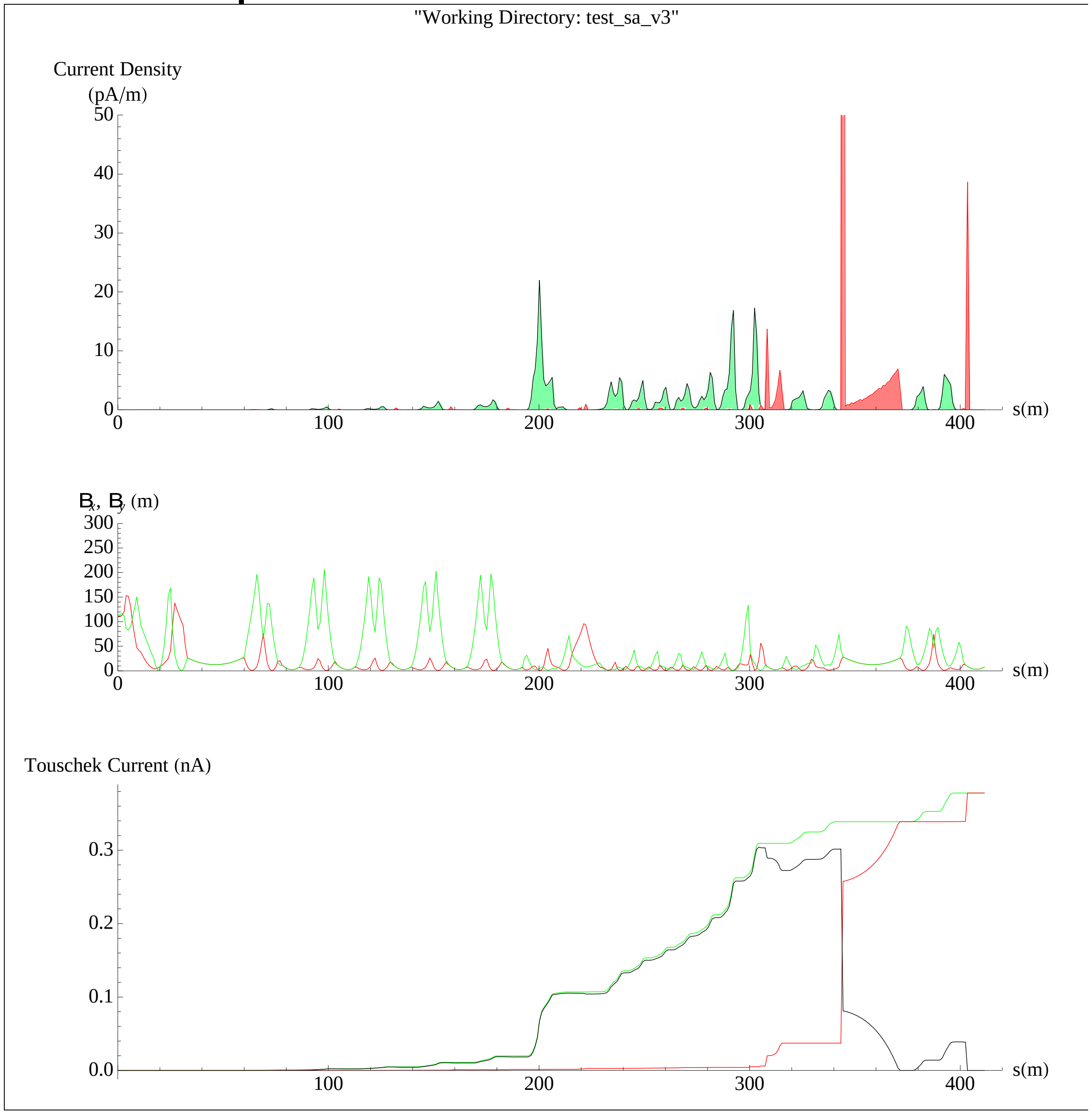

Touschek optimization 3

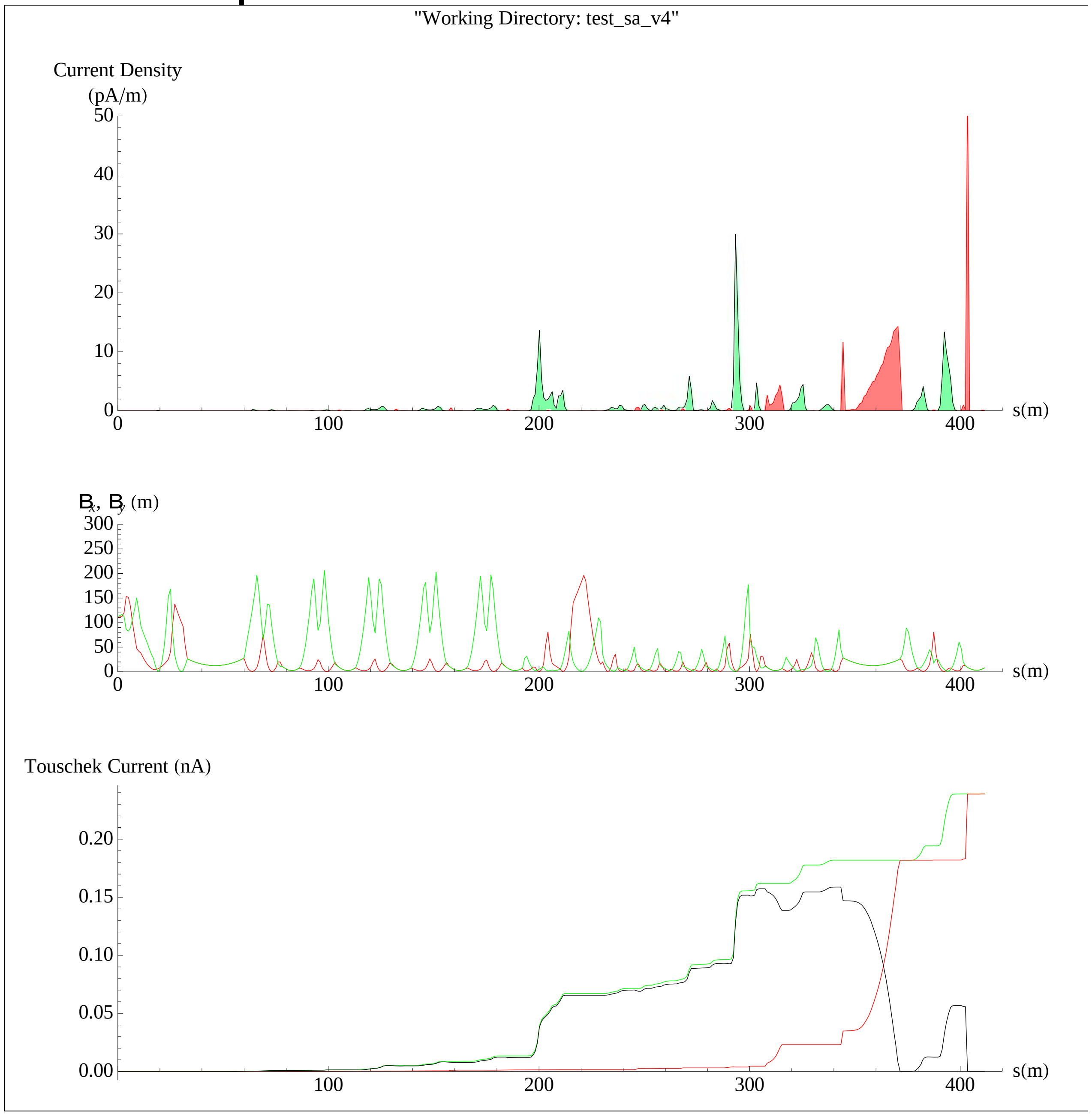

Halo Collimation

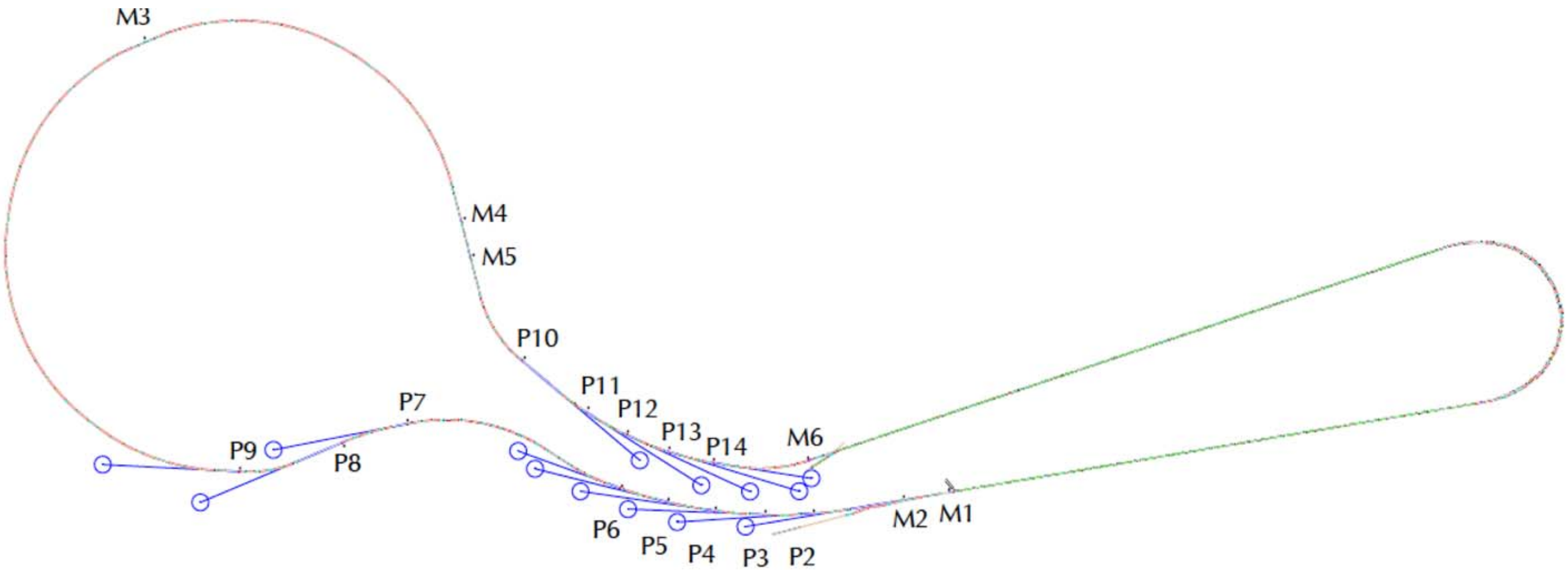

Protector

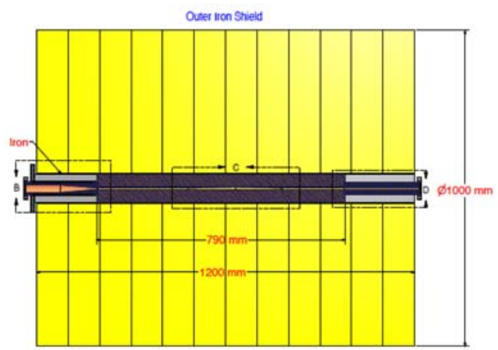

Collimator

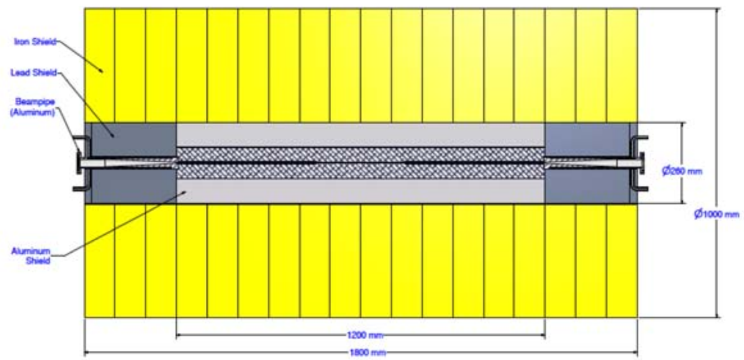

Halo Collimation

Typical Touschek distribution on a collimator face

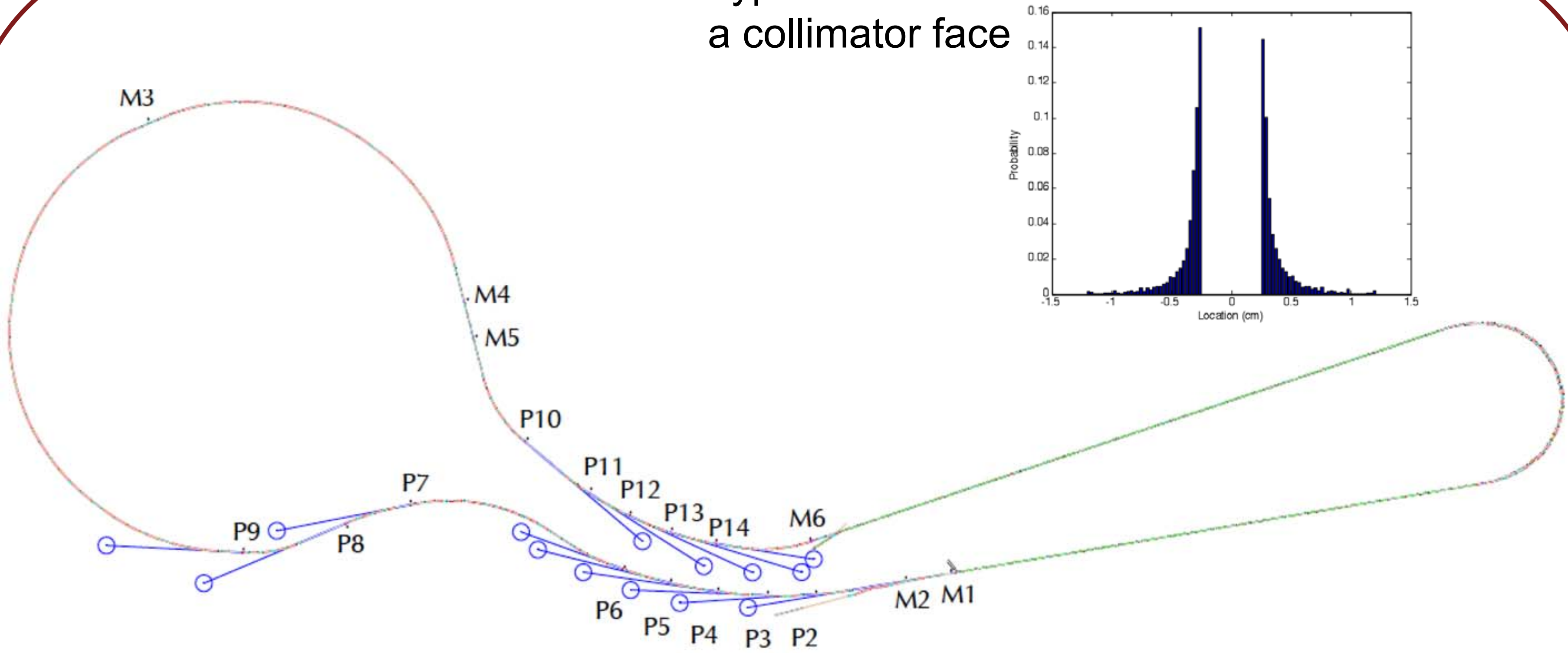

Protector	P2	P3	P4	P5	P6	P7	P8	P9	P10	P11	P12	P13	P14
I(pA)	0	0	0.01	0.37	0.18	46	147	58	1360	0.01	0.04	0.09	0.14

Collimator	M1	M2	M3	M4	M5	M6
I(nA)	31.7	7.85	110	163	136	2.17

Photon Dose Rates (MCNPX)

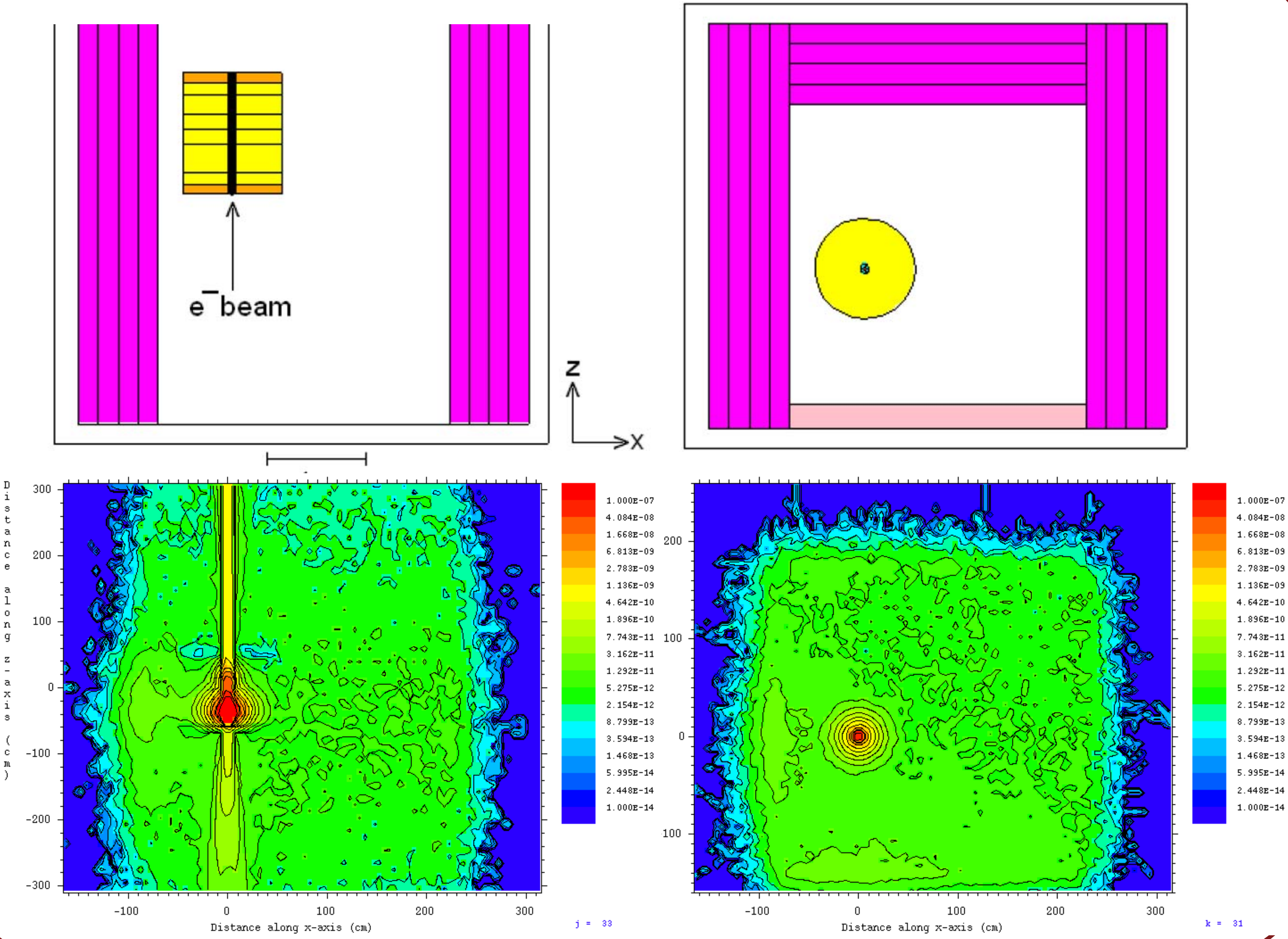

Neutron dose rate contours in (rem/h)/(el/s)

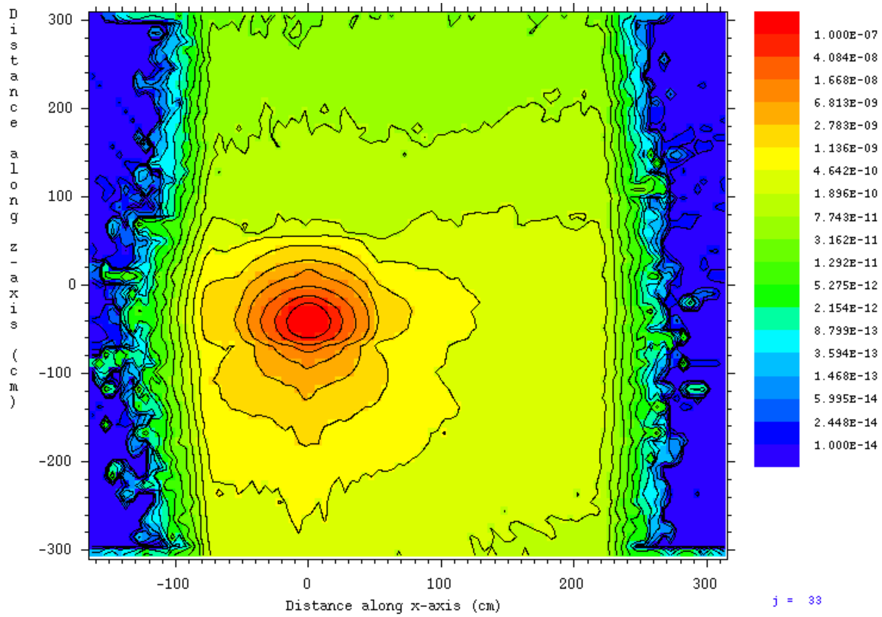

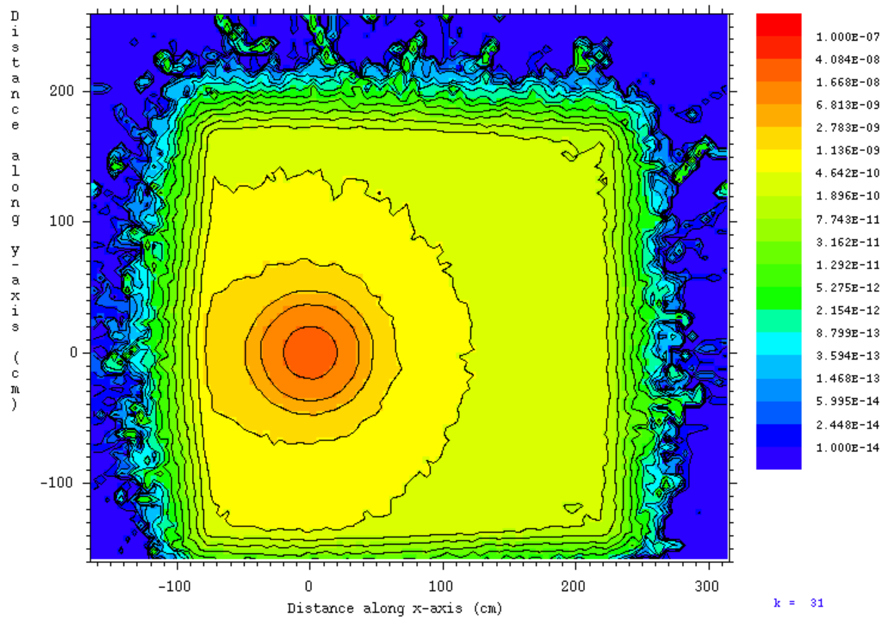

Result:

- no signifigant hazard to personnel
- no signifigant demagnitization of undulator permanent magnets

Touschek halo tracking

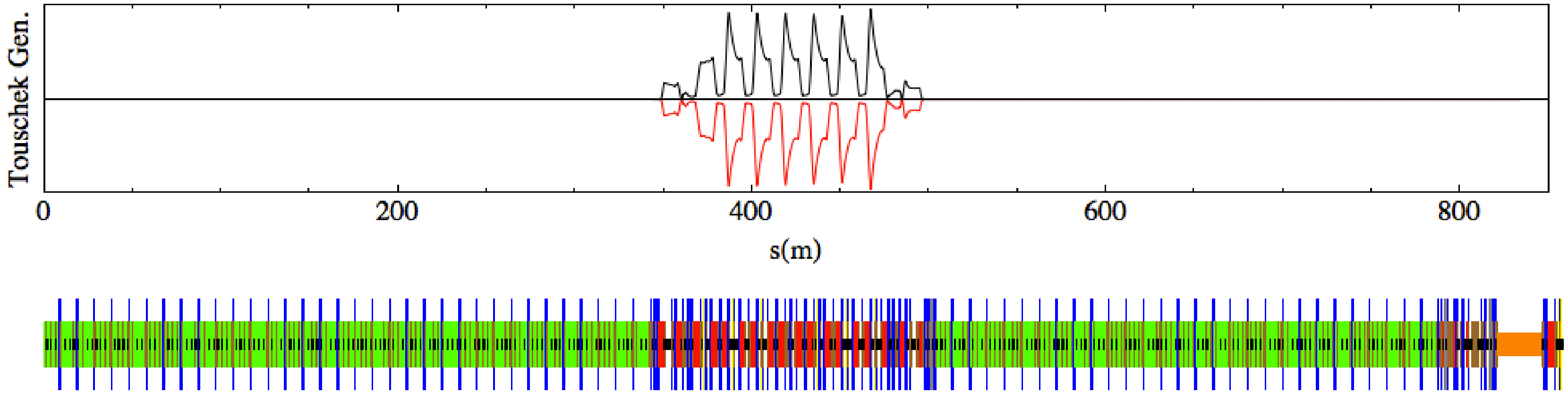

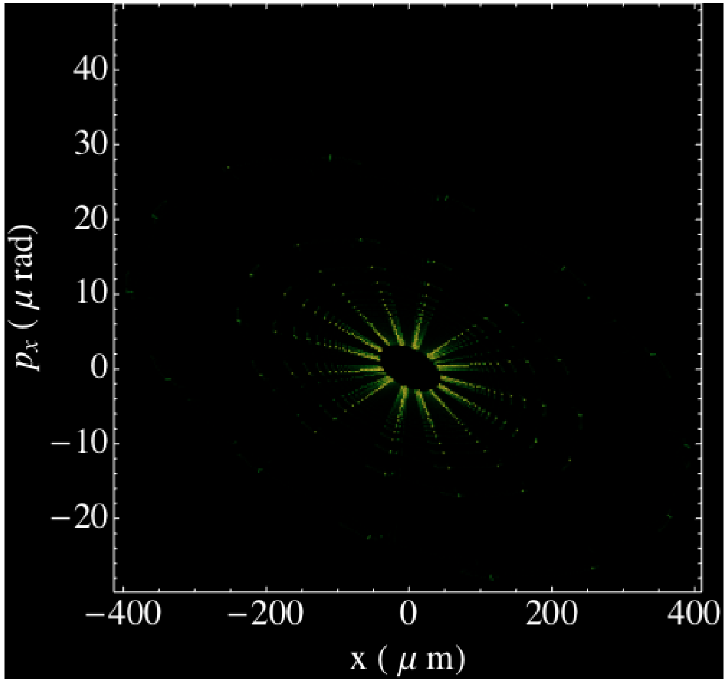

Dark Current Tracking

$$I_{\mathrm{FN}}\left(E_{\perp}\right) = a_0\, A_{\mathrm{FN}}\left(\beta_{\mathrm{FN}} E_{\perp}\right)^2 \exp\left(-\frac{a_1}{\beta_{\mathrm{FN}} E_{\perp}}\right) \qquad Q_n = N_A \cdot A_n \cdot \frac{\Delta\phi_{\mathrm{n}}}{2\pi f_{\mathrm{rf}}} \cdot I_{\mathrm{FN}}(E_{\perp}(t_n))$$

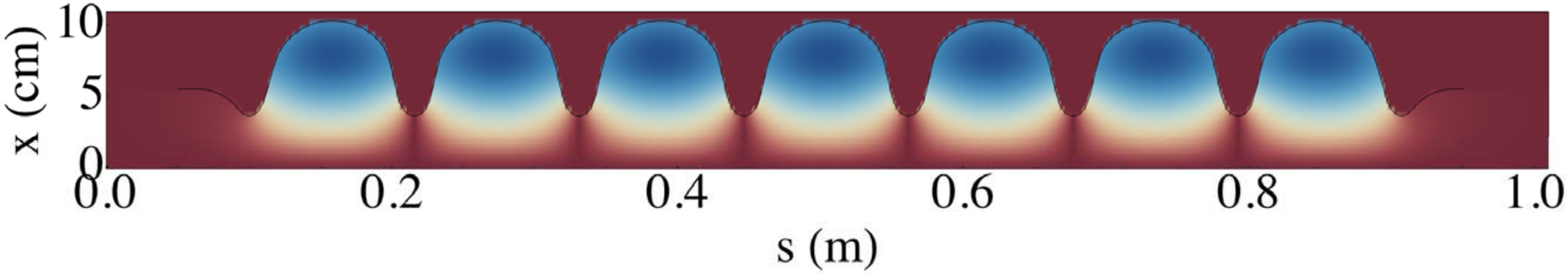

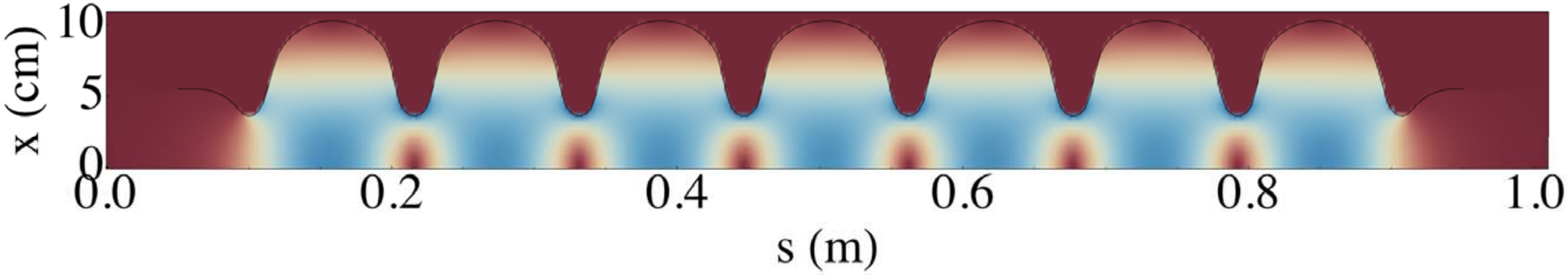

Gamma radiation in test cryomodule (MCNPX)

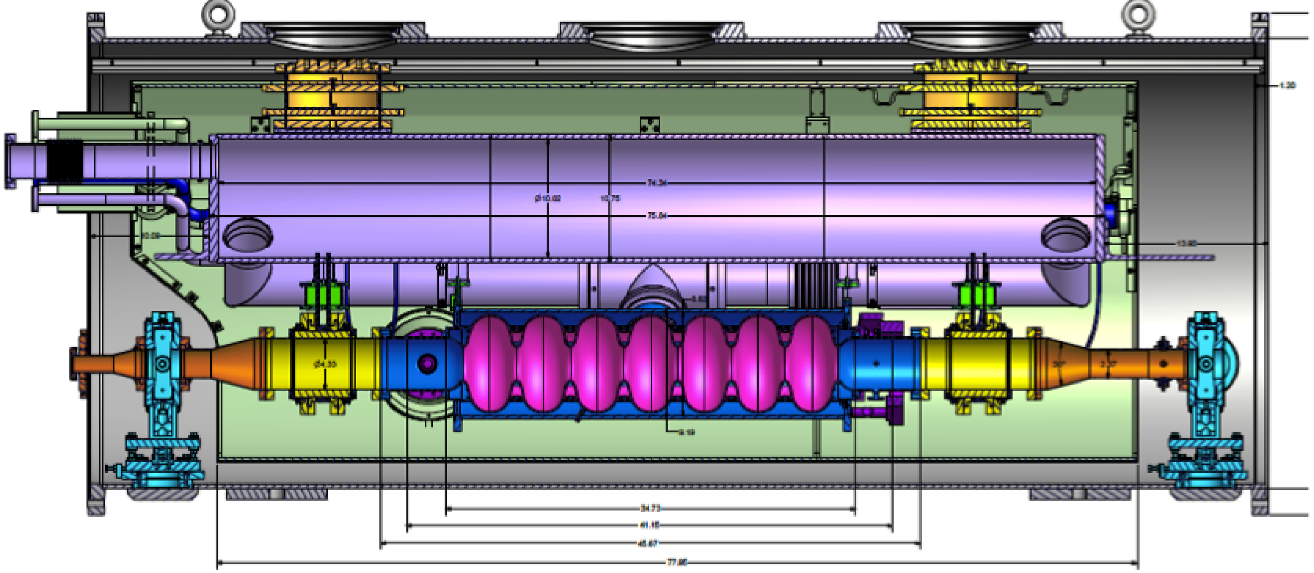

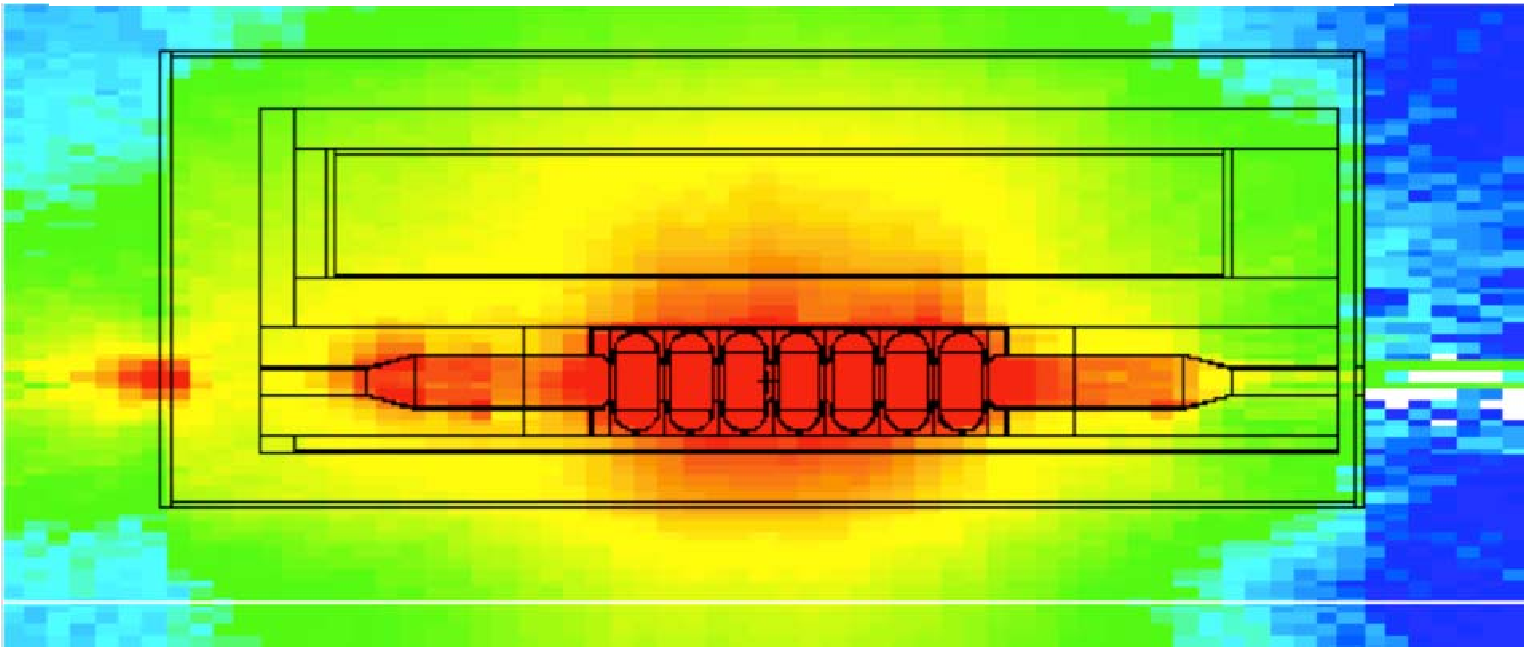

Field emission in two cryomodules

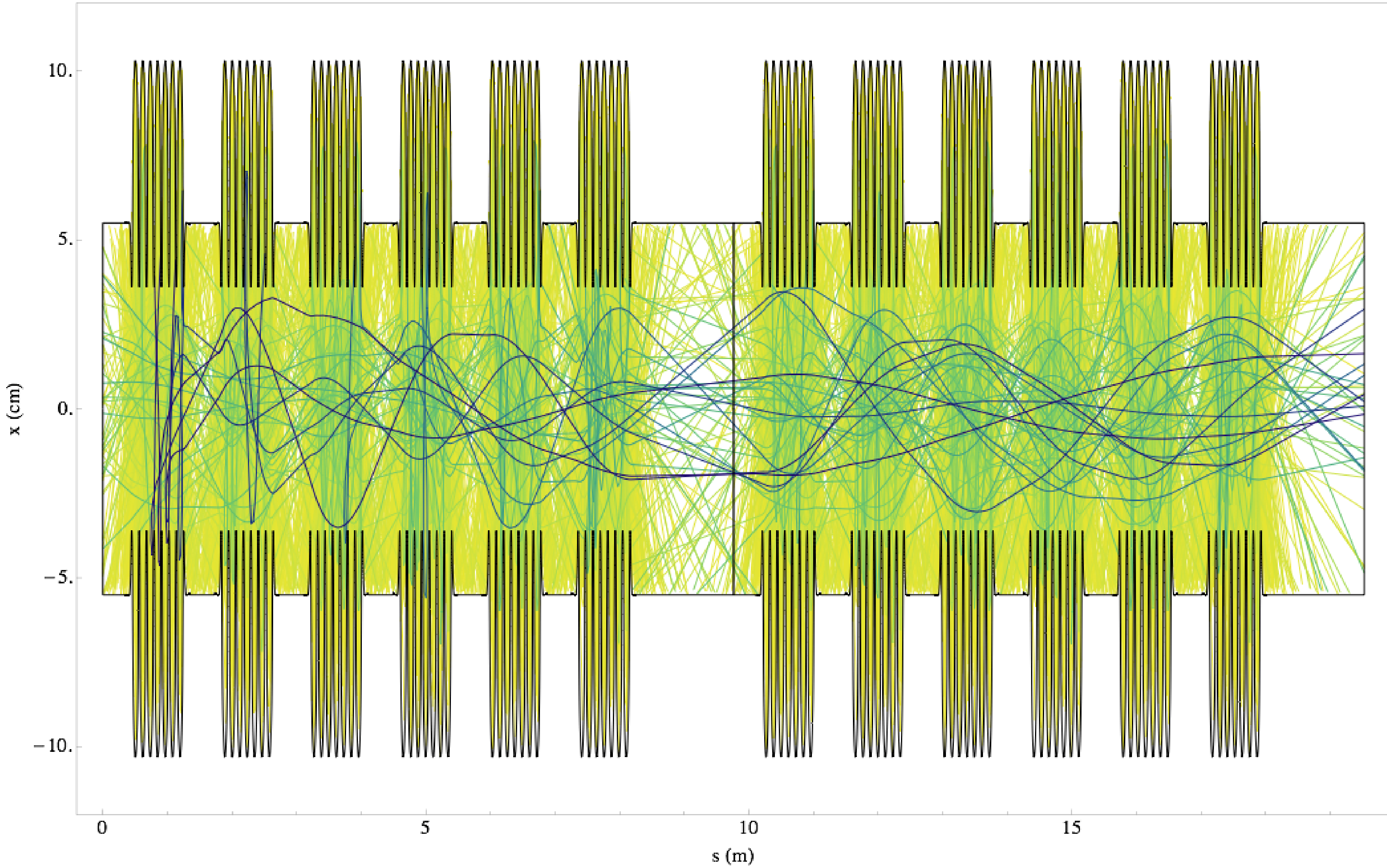

Field emission in one linac

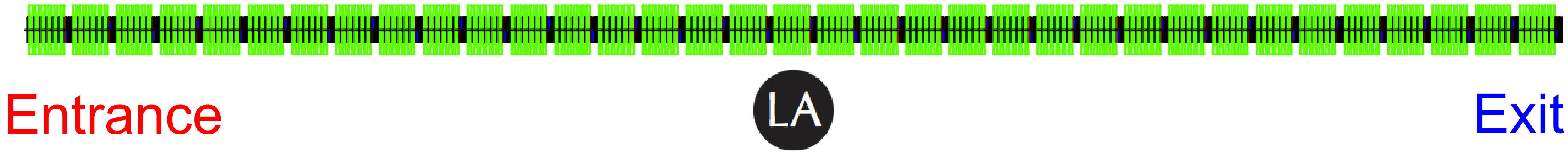

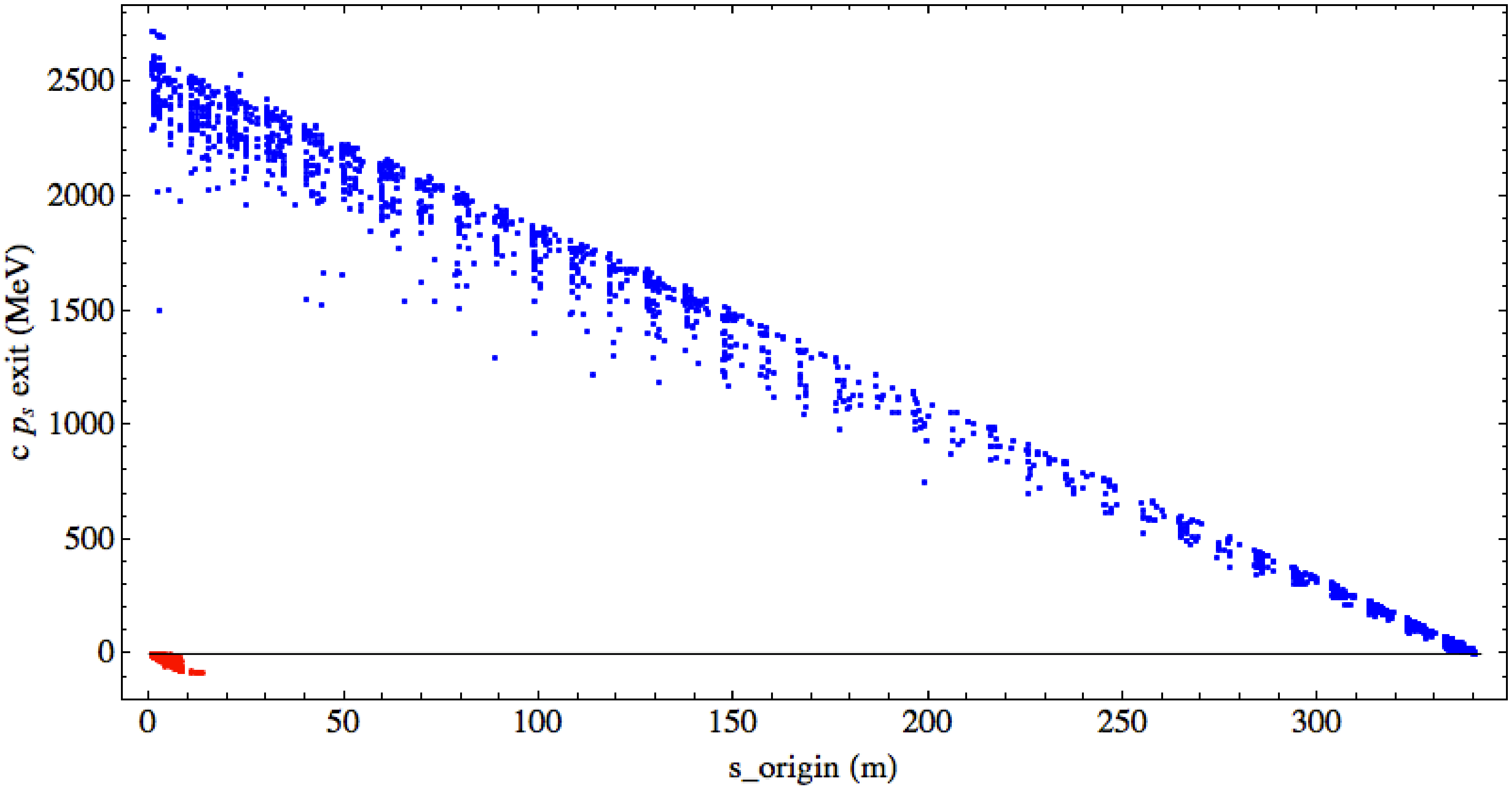

Two cryomodules: Left Exiting particles

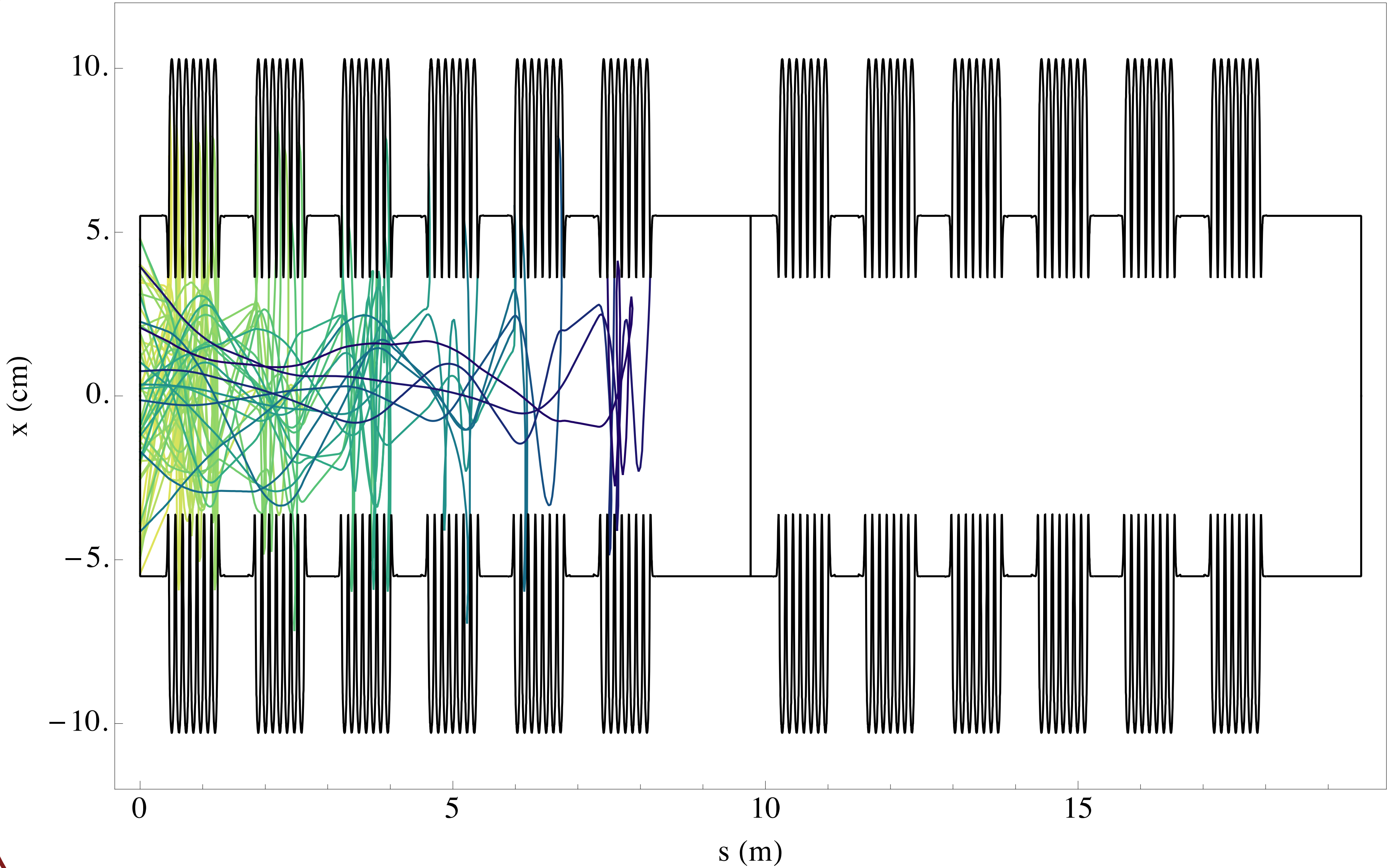

Right exiting particles

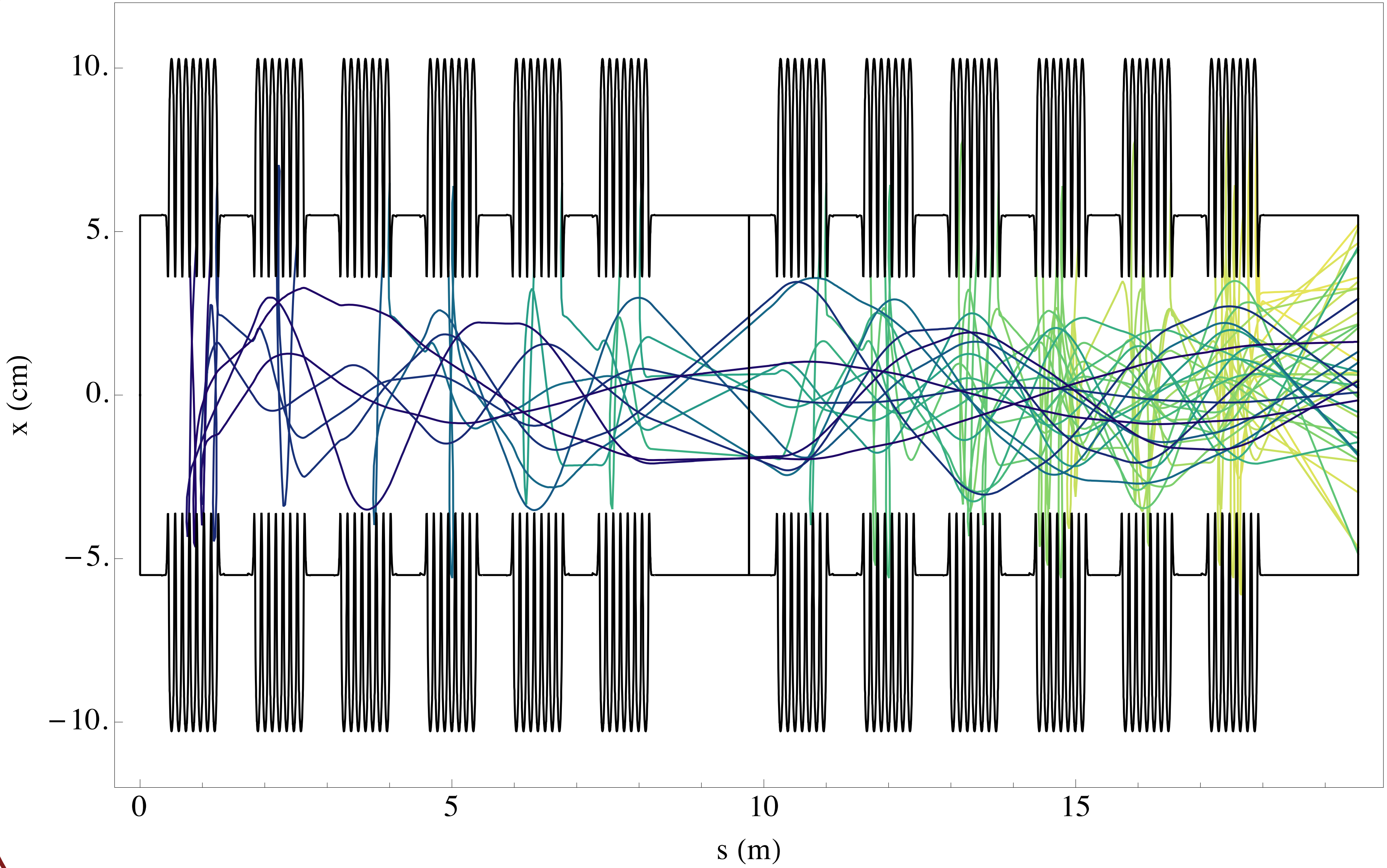

Left moving particles through the center

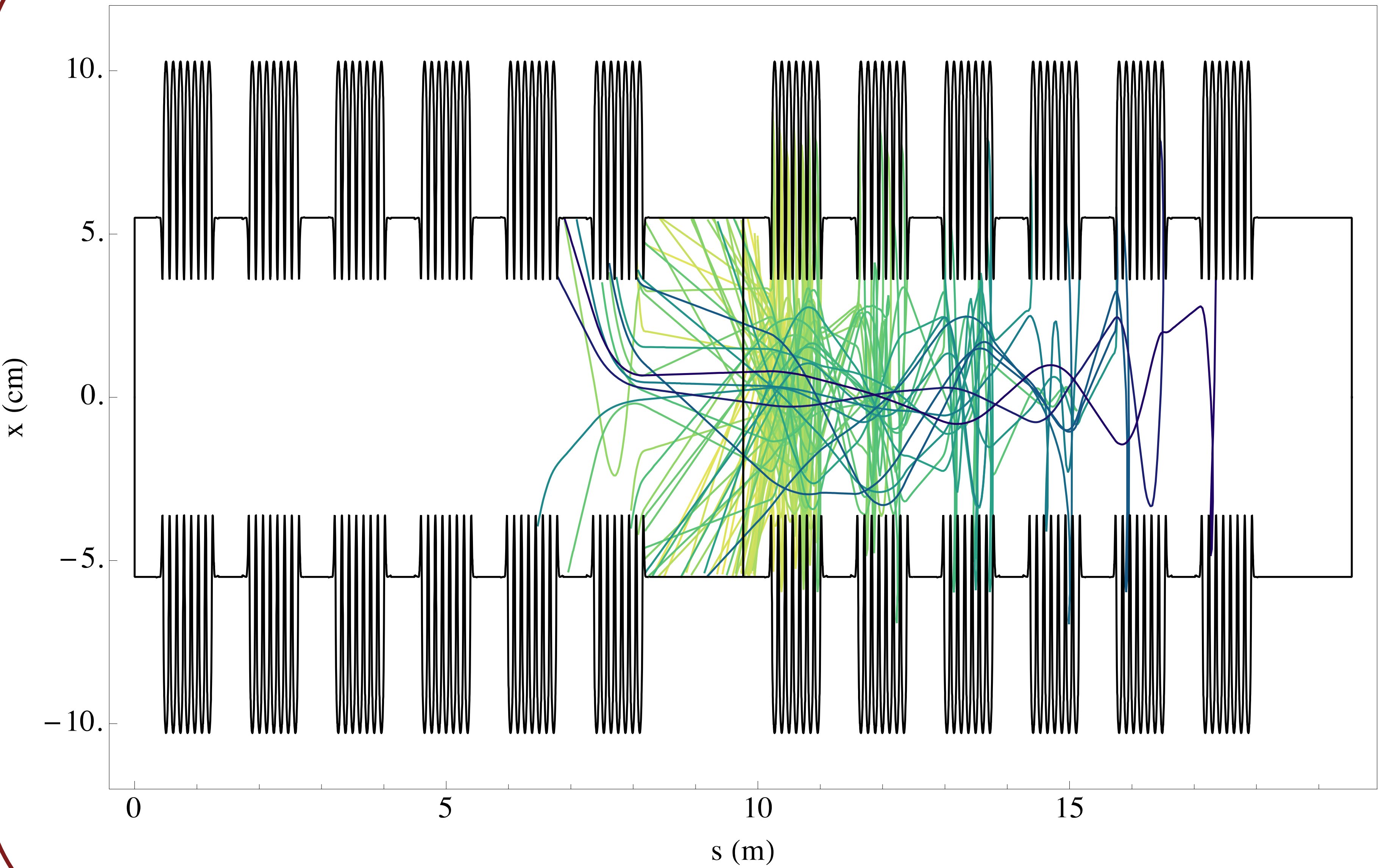

Exit Halo

Energy Distributions

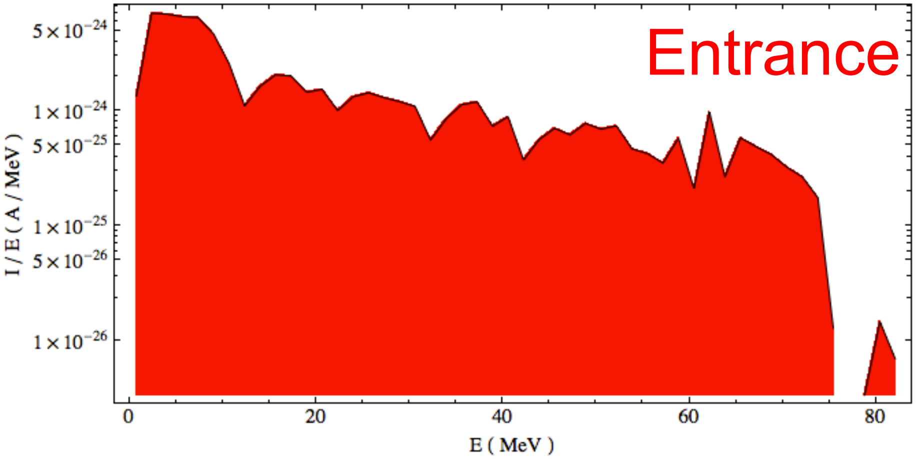

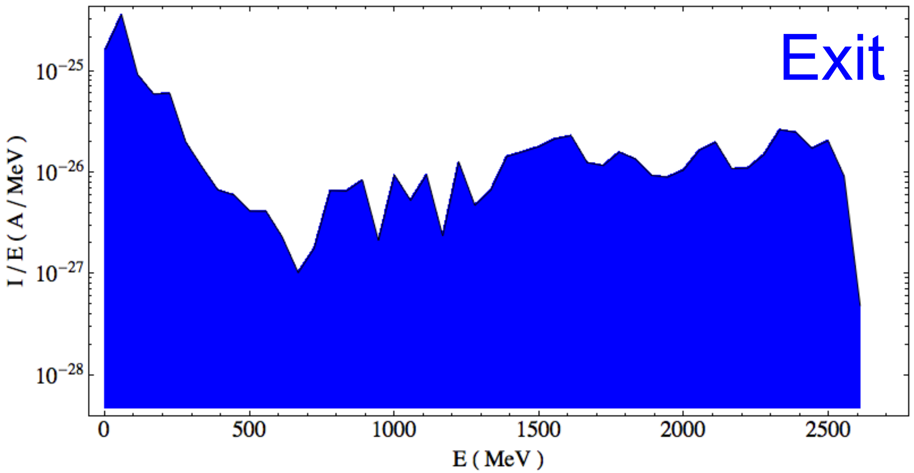

Longitudinal Phase Space

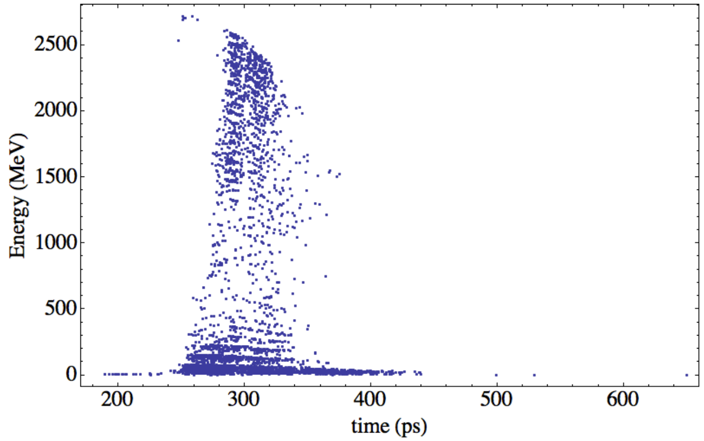

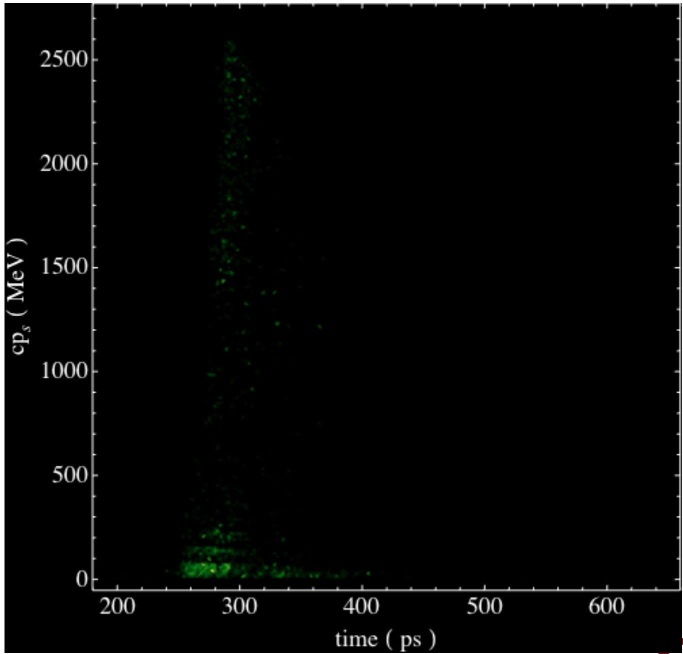

Next steps: secondary emission, . . .

MCNPX calculations on a 3 mm slab of niobium

Electron yield | Electron energy (MeV)

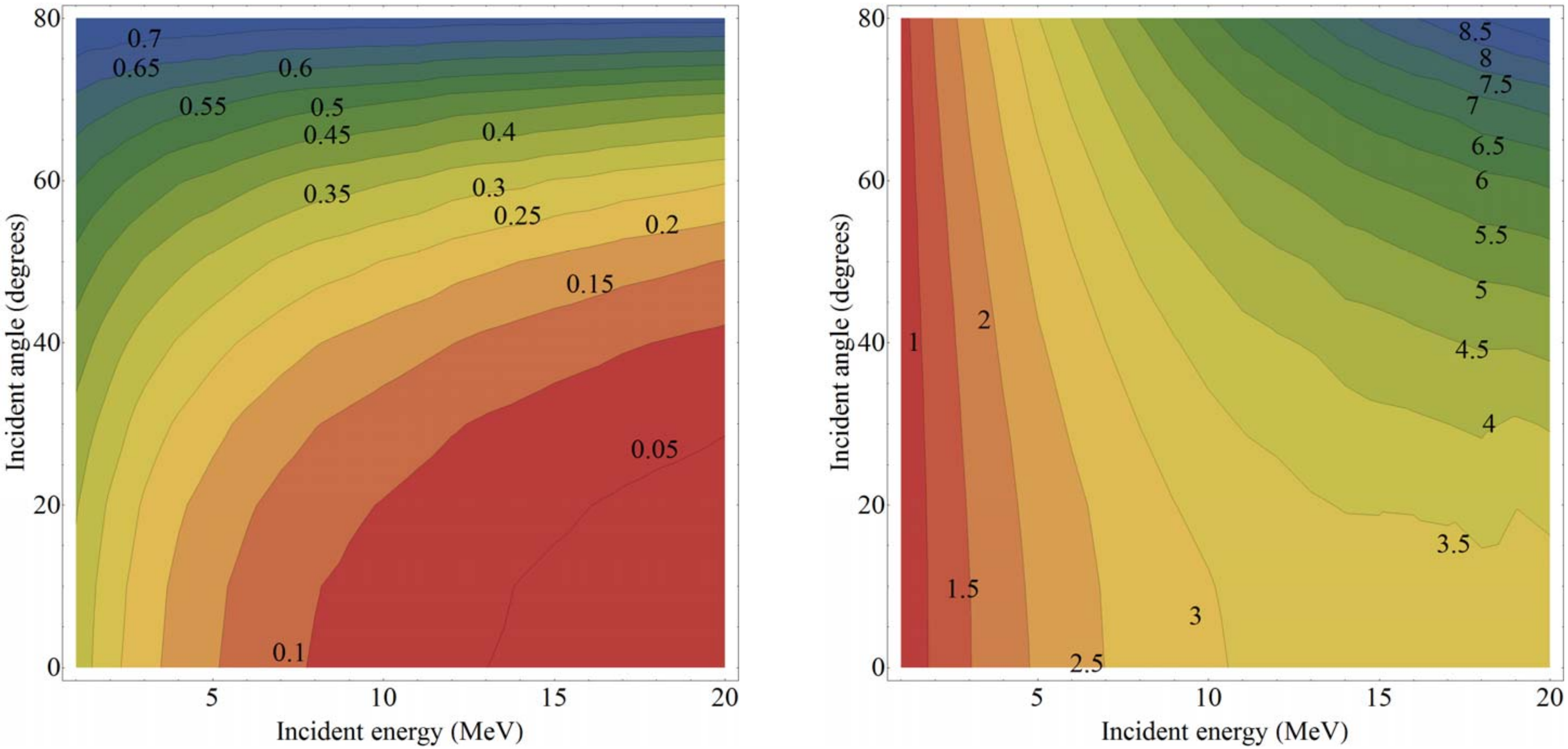

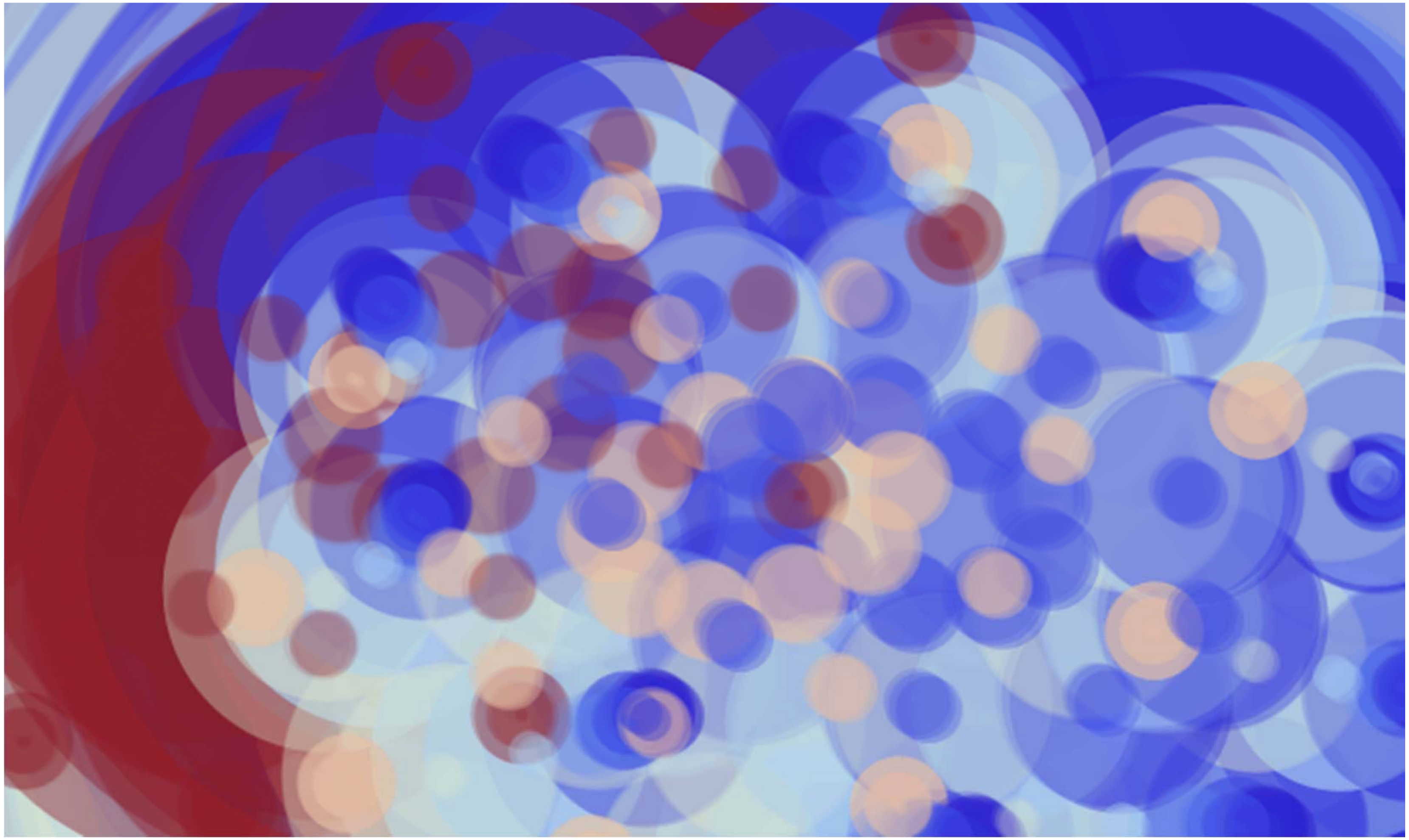

End